

## Light-shift-induced spatial structures: Application to degenerate four-wave mixing

M. Schiffer, E. Cruse, and W. Lange

*Institut für Angewandte Physik, Westfälische Wilhelms-Universität Münster,  
Corrensstrasse 2-4, D-48149 Münster, Germany*

(Received 11 February 1994)

Degenerate four-wave mixing in dense sodium vapor under conditions of strong pressure-induced Zeeman pumping is investigated. Thermal diffusion and its interplay with the Zeeman light shift are found to be responsible for the generation of a grating mechanism that is not sensitive to thermal washout. The effect can be observed experimentally after eliminating the influence of radiation trapping by the use of nitrogen as a buffer gas. Under these conditions large nonlinearities are produced which also influence the propagation of the signal wave via collision-aided circular birefringence.

PACS number(s): 42.65.Hw, 32.80.-t

Resonant degenerate four-wave mixing (DFWM), employing sodium vapor under a buffer gas atmosphere as the nonlinear medium, has been studied over more than a decade and provided a lot of fundamental insight in the process of DFWM. It has, e.g., been used extensively in the study of pressure-induced effects [1–4], where optical pumping processes in the sodium ground state establish a nonlinear behavior which is easily accessible even with low-power cw lasers. However, in this case the nonlinearity of the medium is governed by a long-living physical quantity, i.e., the ground-state orientation, which undergoes thermal diffusion. For oriented sodium atoms diluted in a diamagnetic gas, it is assumed that the orientation is efficiently destroyed only by collisions with the cell walls. The diffusive motion of the oriented atoms should therefore lead to a washout of the contrast of the laser-induced grating, and thus to a reduction of the DFWM signal. The fundamental question then arises, why the diffusive motion of the atoms does not generally destroy the signals, and which physical mechanisms provide the indispensable gratinglike variation of the refractive index.

Recently it has been demonstrated [5] that under conditions of high sodium densities, one possible mechanism responsible for this variation is radiation trapping, which can be viewed as an additional decay process for orientation [6], thus avoiding a complete saturation of the medium by counteracting the effect of thermal diffusion. However, the effect of radiation trapping can be suppressed if the rare gas, usually used in the experiments, is replaced by nitrogen, which collisionally quenches the excited sodium states, but leaves ground-state properties unaffected [7]. Thus even at high sodium densities the influence of thermal diffusion can be reestablished. We study the magneto-optic properties of this system, find that the dependence of the signal on the magnetic field is quite unexpected, and trace back the peculiarities to the effect of the light shift, i.e., we demonstrate that the intensity dependence of the light shift provides a means of sustaining a spatial gratinglike structure. Similar to the effect of radiation trapping, the light shift reduces the effect of thermal washout and dominates the signal characteristics, but in contrast this “light-shift grating”

has a most unusual feature, that it requires the generation and even the diffusion of ground-state orientation in the grating region, but that it is not itself sensitive to a washout. We also demonstrate that under these conditions the collision-aided Faraday effect has a strong influence on the polarization properties of the DFWM signals.

In order to demonstrate the effect of the light-shift grating, we performed experiments similar to those described in Refs. [1,2,5], but used a high sodium density. Our experimental setup makes use of the standard four-wave-mixing geometry schematically depicted in Fig. 1. Sodium in a nitrogen buffer gas atmosphere of typically about 300 hPa is contained in a stainless steel cell with a heated zone of 5 cm in length. The cell temperature can be varied from 200 °C to 320 °C, corresponding to a sodium density of  $5 \times 10^{12}$  to  $2 \times 10^{14}$  cm<sup>-3</sup>. Helmholtz-type coils in three dimensions allow a well defined magnetic field to be applied to the interaction zone. Two circularly polarized ( $\sigma_+$ ) beams from a cw dye laser, with a power of approximately 70 mW each, enter the cell, including an angle of typically 3 mrad. The backward beam of 8 mW, coming from the same laser, is linearly polarized, i.e., it can be decomposed into  $\sigma_-$  and  $\sigma_+$  components of equal intensity. The frequency detuning is about 20 to 30 GHz from the sodium  $D_1$  resonance line. We measured the magnetic field dependence of the DFWM signal by scanning the transverse magnetic field strength  $B_x$  and keeping the longitudinal component  $B_z$  constant, thus yielding Hanle-type spectra (cf. [1]).

The signal intensity as a function of the applied trans-

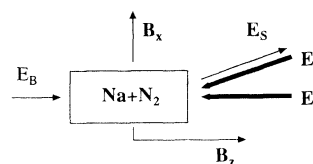


FIG. 1. Experimental scheme: The strong pump beams  $E_1$  and  $E_2$  are circularly polarized, backward  $E_B$  and signal  $E_S$  beams are linearly polarized. The  $B_x$  field is perpendicular to the quantization axis.

verse ( $B_x$ ) and longitudinal ( $B_z$ ) magnetic field is shown in Fig. 2. A complicated asymmetric dependence of the DFWM signal on the longitudinal field is evident. In spite of the high particle density, regions showing the typical saturation dip as reported in Refs. [1,2,5] can be recognized. For other values of the longitudinal field ( $B_z \approx 0.1$  mT), however, also a three peaked spectrum can be observed. It was experimentally confirmed that the  $B_z$  dependence changes sign when the laser is tuned to the other side of the  $D_1$ -resonance line. Figure 3(a) shows the DFWM-signal dependence on  $B_x$ , monitored through a linear polarizer for a given  $B_z$ .

In order to understand the complex behavior of the DFWM signal, the system is described in terms of a density matrix treatment of a  $J = \frac{1}{2} \rightarrow J' = \frac{1}{2}$  model, as shown in Fig. 4. Under the conditions of our experiment, where the hyperfine splitting and Doppler effect can be neglected due to the high buffer gas pressure, this can be regarded as a suitable approximation of the sodium level scheme [8]. The intersecting pump beams generate an interference pattern and create a spatial modulation of the refractive index, from which the backward beam is scattered. The intensity  $I_S$  of the signal wave is proportional to the square of the absolute value of the modulation amplitude of the index grating [9]. In case of negligible excited state population, the refractive index is a linear function of the ground-state orientation  $w = \rho_{22} - \rho_{11}$  leading to a signal intensity:

$$I_S \sim |\delta w|^2. \quad (1)$$

Here  $\delta w$  denotes the difference between the orientation in the maxima and minima of the sinusoidal interference pattern and may be called the modulation amplitude. Applying a transverse magnetic field generates Zeeman coherences  $\rho_{12}$  between the sublevels of the ground state and leads to Hanle-type spectra for the output signal. For the calculation of the signal intensity, the equations for the density matrix elements have to be solved in a space-dependent formulation. This is performed in a one-

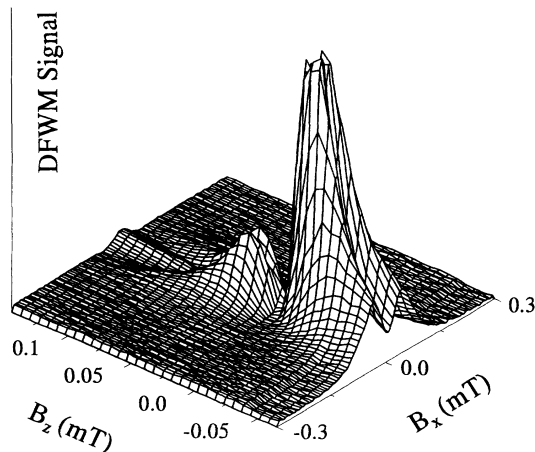


FIG. 2. Magnetic field dependence of the DFWM signal (normalized). Temperature 304 °C;  $p_{N_2} = 380$  mbar; detuning  $\Delta = 25$  GHz.

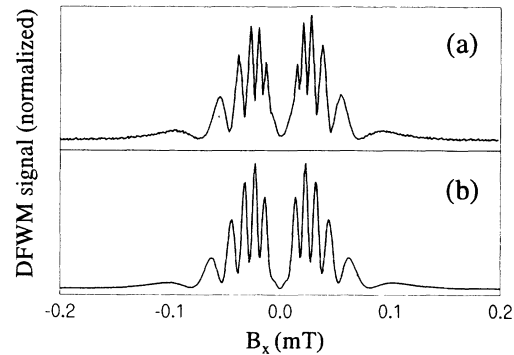


FIG. 3. (a) DFWM signal monitored through a linear polarizer. Temperature 300 °C;  $p_{N_2} = 300$  mbar; Detuning  $\Delta = +25$  GHz. (b) Theory: fit parameters are absorption coefficient and width of the Hanle resonance.

dimensional treatment in terms of the magnetic Bloch vector formalism for the four-level system [10]. A space-dependent pump rate  $P_+(\mathbf{x})$  describes the influence of the strong circularly polarized pump beams and the  $\sigma_+$  component of the backward beam, whereas a much smaller additional pump rate  $P_-(\mathbf{x})$  accounts for the  $\sigma_-$  component of the backward beam. With a detuning  $\Delta$  and a dephasing time for the optical coherence of  $1/\Gamma_2$ , this leads to the following equation for the ground-state magnetization vector  $\mathbf{m} = (u, v, w)$ , where  $\Omega_{x,z}$  denote the Larmor frequencies produced by the  $B_x$  and  $B_z$  component of the magnetic field, respectively:

$$\dot{\mathbf{m}}(x, t) = \boldsymbol{\Omega} \times \mathbf{m} - \gamma_{\text{eff}} \mathbf{m} + D_{\text{th}} \nabla^2 \mathbf{m} + \mathbf{P}, \quad (2)$$

with

$$\boldsymbol{\Omega}(x) = \left( \Omega_x, 0, \Omega_z - \frac{\Delta}{\Gamma_2} (P_+ - P_-) \right), \quad (3)$$

$$\mathbf{P}(x) = (0, 0, (P_+ - P_-)) \quad (4)$$

$$\gamma_{\text{eff}} = P_+ + P_-. \quad (5)$$

In these equations, the diffusion term describes the spatial evolution of oriented atoms. For a determination of the boundary conditions, it is assumed that oriented atoms become disoriented at the cell walls, thus introducing an overall loss of orientation. The contribution  $-\frac{\Delta}{\Gamma_2} (P_+ - P_-)$  to the  $z$  component of  $\boldsymbol{\Omega}$  represents the well-known light shift. For the calculation of the signal intensity according to Eq. (1), the stationary space-dependent solution for a simplified one-dimensional for-

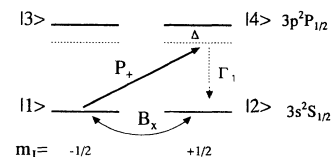


FIG. 4. Schematic of the four-level model. The pump beams induce optical pumping between the Zeeman sublevels with a pump rate  $P_+$ . A transverse magnetic field couples the Zeeman sublevels. The natural lifetime of the excited state is  $1/\Gamma_1$  and the detuning is denoted by  $\Delta$ .

mulation of Eq. (2) is computed.

A result for the magnetic field dependence is shown in Fig. 5. The qualitative agreement with the experimental curves is striking.

The results can be interpreted if thermal diffusion and the light shift are considered. In the spatial regions where constructive interference between the two pump beams occurs, the light shift produces a fictitious longitudinal component of the magnetic field which adds up with the applied external magnetic fields to form a gratinglike variation of the effective magnetic field. This variation of the effective magnetic field is stationary in space and may be called a light-shift grating. In the maxima of the interference pattern, optical pumping leads to the generation of a magnetization vector, which points in a direction determined by the local effective magnetic field.

The orientation  $w$ , which is the quantity to form the refractive index, is the projection of the magnetization vector  $\mathbf{m}$  on the quantization axis. As the direction of the magnetization vector is determined by the effective magnetic field, the value of this projection changes, if atoms bearing a certain magnetization move from the regions with additional light-shift-induced components of the effective magnetic field (the maxima of the interference grating) to the regions where only the applied static field is present (the minima of the grating). Due to the negligible destruction of magnetization inside the interaction volume, only this mechanism is responsible for the index modulation.

The relative influence of the light-shift-induced grating is dependent on the detuning and on the sign and strength of the applied  $B_z$  field and is most distinct in the vicinity of the zero field region, when detuning and applied  $B_z$  field have the same sign, which leads to a strong difference in the effective magnetic field between maxima and minima of the grating, thus resulting in the strong maximum. The diffusion of oriented atoms into the minima of the grating, where a different magnetic field is present can even result in a change of the sign of the orientation difference at some values of the trans-

verse field. This is the case if the light-shift term has the sign opposite the applied  $B_z$  field and reduces the longitudinal component in the maxima of the grating, which in turn enhances the influence of the coherence generated by the transverse field and reduces the orientation in this region. In the minima of the grating, however, the longitudinal component may be still large enough to preserve the orientation, thus changing the sign of the modulation amplitude. Scanning the transverse field then leads to the observed three-peaked spectra, where the minima refer to zero crossings of the modulation amplitude, i.e., the sign of  $\delta w$  changes. A change of the detuning from the red to the blue side of the resonance line changes the sign of the light-shift-induced part of the effective longitudinal magnetic field and results in the inversion of the  $B_z$  dependence, as was observed in the experiment.

As can be inferred from this discussion, the interplay between thermal diffusion, light-shift grating, and external magnetic fields leads to unexpected features of the DFWM process, which become manifest in the three-peaked spectra and strong asymmetries in the magnetic field dependence. It has to be stated that the inclusion of the diffusion term in the Bloch equations is fundamental for the correct modeling of the system behavior. If the diffusion term is replaced by an exponential decay rate, the results of the calculations no longer show any similarity to the experimental results.

An explanation for the complex spectra of Fig. 3(a) is obtained by considering that the DFWM signal intensity is determined by the modulation of the refractive index (given by  $\delta w$ ), but that the propagation of the signal beam inside the medium can be influenced by the absolute value of  $n$  (given by  $w$ ). Following the argument that in the sodium-nitrogen system destruction of orientation is only achieved at the cell walls, the sample may be almost completely oriented in the zero-transverse-field region with a small light-shift-induced variation of the refractive index leading to the signal output. While propagating through the saturated medium of length  $l$ , collision-induced circular birefringence [11,12] rotates the plane of polarization of the linearly polarized signal beam. The detected signal is proportional to

$$I_{\text{det}} \sim I_S(B_x) \sin^2(\Theta) \quad (6)$$

with the Faraday rotation angle for a particle density  $N$  being

$$\Theta \sim (n_+ - n_-) \sim lNw. \quad (7)$$

The signal shape  $I_S(B_x)$  was computed with the above model. An example for the magnetic field dependence calculated according to Eq. (3) is given in Fig. 3(b). This calculation includes signal beam absorption, which leads to a slightly elliptically polarized signal beam in the experiment, as the sample is strongly oriented and the  $\sigma_-$  component of the linear polarized signal beam is partially absorbed. Every maximum in the spectrum is related to a rotation angle of  $180^\circ$ , indicating a rotation angle of about  $1080^\circ$  induced by the strong interaction between the dense vapor and the propagating signal wave.

In conclusion the influence of the light-shift grating on the characteristics of the DFWM signal presents a

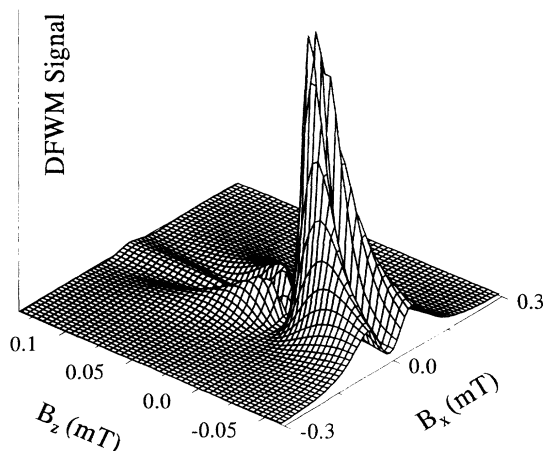


FIG. 5. Calculated intensity of the signal wave for the experimental parameters of Fig. 2.

striking example for the influence of diffusion processes on DFWM experiments. For a complete description of four-wave-mixing processes in systems with nonlinearities based on long-lived quantities, the interpretation of experimental results has to consider thermal motion and its interplay with external parameters. The influence of thermal diffusion may not only lead to washout effects, but it may affect the nonlinear behavior in a more subtle way. Our investigations also reveal very clearly that the approximation of pure exponential decay for long-lived

contributions to the nonlinearity is by no means applicable in every case. Furthermore, we would like to point out that the light-shift-induced variation of the refractive index, which is proportional to the resulting intensity distribution of the input beams, can play its role in all experiments that depend on the spatial dependence of the nonlinear polarization of the medium. One example is the formation of transverse patterns which result from the nonlinear interaction of a laser beam with Gaussian intensity distribution and sodium vapor [13].

- 
- [1] Y.H. Zou and N. Bloembergen, *Phys. Rev. A* **34**, 2968 (1986).
  - [2] E. Köster, J. Mlynek, and W. Lange, *Opt. Commun.* **53**, 53 (1985).
  - [3] Y.H. Zou and N. Bloembergen, *Phys. Rev. A* **33**, 1730 (1986).
  - [4] G.S. Agarwal, *Adv. Atom. Mol. Opt. Phys.* **29**, 113 (1991).
  - [5] M. Schiffer, G. Ankerhold, E. Cruse, and W. Lange, *Phys. Rev. A* **49**, 1558 (1994).
  - [6] G. Ankerhold, M. Schiffer, D. Mutschall, T. Scholz, and W. Lange, *Phys. Rev. A* **48**, R4031 (1993).
  - [7] A.C. Tam, *J. Appl. Phys.* **50**, 1171 (1979).
  - [8] D. Suter, *Phys. Rev. A* **46**, 344 (1992).
  - [9] H.J. Eichler, P. Günter, and D.W. Pohl, *Laser-Induced Dynamic Gratings* (Springer-Verlag, Berlin, 1986).
  - [10] F. Mitschke, R. Deserno, W. Lange, and J. Mlynek, *Phys. Rev. A* **33**, 3219 (1986).
  - [11] M. Pinard, P. Verkerk, E. Giacobbono, and G. Grynberg, *Phys. Rev. A* **35**, 2951 (1987).
  - [12] Q. Gong and Y.H. Zou, *Opt. Commun.* **66**, 294 (1988).
  - [13] A. Gahl and W. Lange (unpublished).